frontiers in Earth Science

ORIGINAL RESEARCH
published: 07 August 2020
doi: 10.3389/feart.2020.00323

Pyroclastic Density Current Facies in the Millennium Eruption of Tianchi Volcano, Northeast China: Insights From Topography, Stratigraphy, Granulometry, and Petrography

Bo Zhao[1,2], Jiandong Xu[1,2], Hongmei Yu[1,2] and Zhengquan Chen[1,2]*

[1] National Observation and Research Station of Jilin Changbaishan Volcano, Institute of Geology, China Earthquake Administration, Beijing, China, [2] Key Laboratory of Seismic and Volcanic Hazards, Institute of Geology, China Earthquake Administration, Beijing, China

Large-scale pyroclastic density currents (PDCs) produce inhomogeneity of distributions, thicknesses, stratigraphic structures, and temperatures, thereby causing poor understanding of PDC emplacement processes. Millennium Eruption (ME) of Tianchi volcano in 946 A.D. produced masses of PDCs, covering an area of more than 1570 km^2 around the caldera in the Chinese territory. To understand PDC emplacement processes, we examine the proximal to distal variations in the PDC facies during the ME by analyzing the topography, stratigraphy, granulometry, and petrography. The topography of Tianchi volcano has different slopes, including the cone (> 6°), lava shield (2–5°) and lava plateau (< 1°), which affected the PDC emplacement during the ME. The shape of the PDC deposits radiates outward from the caldera, and the periphery has two pyroclastic aprons. The proximal strata (< 10 km) are less than 4 m thick and consist of eutaxitic and lava-like structures in the gullies of the cone. The medial strata (10–20 km) are 10–60 m thick, with columnar joints, pumice-rich layers, and lithic-rich layers in the valleys of the shield. The distal strata (> 20 km) are less than 10 m thick, with coarse-tail layers, ground surge layers, climbing layers, and carbonized woods in the plateau. From the proximal to the distal strata, the emplacement temperature of the PDCs decreased from 740 to 280°C. The medial layers indicate a gravitational differentiation effect and weakened transportation, which led to the formation of thick beds. The distal PDCs demonstrate fluidization characteristics and a density lower than that of the proximal and medial strata, which exhibit clear stratification. Grain size data (< 64 mm) show that the median diameters decreases with increasing distance from the caldera. Rhyolitic and trachytic pumice were found and are assumed to be associated with the composition of the magma chamber. Magmatic mixing structures were confirmed through microscope observations. The volume of the PDCs in the Chinese territory is approximately 7 km^3. Our results assist in unraveling some PDCs emplacement processes, marked by a high level of topography confinement, about 50 km runout distance, 280–750°C emplacement temperatures, and more than 7 km^3 volume, which provide insights of the PDCs destruction during the ME.

Keywords: Tianchi volcano, Millennium Eruption, PDCs, facies, topography

OPEN ACCESS

Edited by:
Pablo Tierz,
The Lyell Centre, United Kingdom

Reviewed by:
Sonia Calvari,
National Institute of Geophysics and Volcanology, Italy
Micol Todesco,
Istituto Nazionale di Geofisica e Vulcanologia (INGV), Italy

****Correspondence:***
Bo Zhao
zhaobo@ies.ac.cn

Specialty section:
This article was submitted to Volcanology, a section of the journal Frontiers in Earth Science

Received: *17 February 2020*
Accepted: *13 July 2020*
Published: *07 August 2020*

Citation:
Zhao B, Xu J, Yu H and Chen Z (2020) Pyroclastic Density Current Facies in the Millennium Eruption of Tianchi Volcano, Northeast China: Insights From Topography, Stratigraphy, Granulometry, and Petrography. Front. Earth Sci. 8:323. doi: 10.3389/feart.2020.00323

INTRODUCTION

Large-scale eruptions, characterized by volcanic explosivity index (VEI) $\geq$ 7, always produce masses of pyroclastic density currents (PDCs), which are one of the most hazardous eruptive phenomena owing to their complex emplacement processes. These PDC deposits are always inhomogeneous in their distributions, thicknesses, stratigraphic structures, and temperatures from the eruptive center to the distal (Branney and Kokelaar, 2002). The emplacement processes of PDCs from large-scale eruptions are still not well understood because these eruptions have not been observed in historic times (Lesti et al., 2011). A useful approach to understanding the emplacements of PDCs from large-scale eruptions is to build a facies model.

Tianchi volcano (also known as Changbaishan or Baitoushan) is a giant intraplate stratovolcano (Wei et al., 1997) that is located on the border between China and North Korea and the Hunchun-Yalu River tectonic fault zone (**Figure 1A**; Liu et al., 1998). The Tianchi caldera has an irregular shape, is 4.4 km from north to south, and 3.3 km from east to west. The highest peak, named Baitou or Jiangjun, has an elevation of 2749 m and is located in North Korea. In 946 A.D., Tianchi volcano experienced a VEI 7 eruption (Xu et al., 2013; Oppenhimer et al., 2017; Pan et al., 2017a) that is known as the Millennium Eruption (ME), which is considered to be one of the largest eruptions on Earth in the last 2000 years (Horn and Schmincke, 2000; Liu, 2000; Wei et al., 2004a). The ME resulted in massive PDCs with a volume of 8.5 km^3 and flowing at a distance of 50 km (Liu and Xiang, 1997a). Historical records suggest that Tianchi volcano may have erupted again in 1199–1200, 1668, 1702, and 1903 after the ME (Jin and Cui, 1999). Currently, the Tianchi caldera lake has stored nearly 2 billion cubic meters of water and has a gap in its northern reaches, which are located in the Chinese territory (**Figure 1B**).

Tianchi volcano has experienced shield-forming, cone-forming, and ignimbrite-forming stages (Liu, 2000; Fan et al., 2006; Wei, 2014). The shield-forming products of Tianchi volcano mainly consists of a basaltic lava plateau around the volcano, formed in 1.2–2 Ma. The cone-forming eruption stage was dominated by trachyte magma, which erupted between 0.1 and 1 Ma. Previous studies generally determined the positions of the cone, lava shield, and lava plateau according to lithological features, leading to different views. Liu (2000) suggested the cone base at an altitude greater than 1600 m. Luan (2008) reported that an altitude of the Tianchi volcanic cone base was more than 1500 m. whereas Wei (2014) stated that a cone base altitude was between 1000 and 1900 m. This discrepancy is caused because different positions of trachytes at the base of the cone were used in these studies. In the last 100,000 years, numerous explosive eruptions have occurred (Jin and Zhang, 1994), with the ME being the best known. The magma is mainly composed of rhyolite. The ME of Tianchi volcano was a Plinian eruption that had an eruption column estimated to be as high as 35 km according to eruption dynamics (Wei et al., 1998). Volcanic ash drifted 1000 km eastward to Japan (Machida and Arai, 1983; Yu et al., 2013), and the eruption column collapsed to form PDCs that cover 2180 km^2 in China (Liu and Xiang, 1997a). Horn and Schmincke (2000) estimated that the magma volume of the eruption was 25 $\pm$ 5 km^3, and divided the ME into an early large-scale eruption (95% volume) and a late small-scale eruption (5% volume), with a 25 km high column of the former. The above information suggests that the ME had a large scale and was complex.

Monitoring data from 2003 to 2006 showed unrest (Ji et al., 2009; Stone, 2010; Liu et al., 2011; Xu et al., 2012; Wei et al., 2013). The background value of the seismic events was 2 per month in Tianchi volcano before 2003 (Liu et al., 1992, 2011; Li and Sun, 1996; Xu et al., 2012). The number increased to 72 per month from 2003 to 2006, with a maximum of 243 in 1 month. The annual average horizontal displacements away from the caldera were 19.6 mm/yr from 2002 to 2003, 10.2 mm/yr from 2003 to 2004, and 8.6 mm/yr from 2004 to 2005. The average $^3He/^4He$ ratio of a hot spring in the Changbaishan valley, 3.57 km away from the center of the caldera lake, was approximately 6.5 between 2003 and 2006, which is higher than before 2003 (average ratio of 5.35). After 2006, the monitoring data showed a return to the level before 2003. This monitoring evidence shows the potential of a future eruption at Tianchi volcano. PDCs are the most hazardous volcanic phenomena for the population living near the volcano due to their large dynamic pressure, fast velocity, long run-out distance and high temperature (e.g., Druitt, 1998; Branney and Kokelaar, 2002; Sulpizio et al., 2014; Dufek et al., 2015). Loose deposits of PDCs are also the main particle sources for secondary lahars, which can occur during non-eruptive periods (e.g., Blong, 1996; Pierson and Major, 2014). Therefore, it is important to identify lithofacies characteristics, such as the spatial distribution, thickness, grain size, and stratigraphic structures of PDCs produced during the ME, to better understand the eruption dynamics and provide a reference for emergency plans to reduce casualties and property loss.

Researchers have investigated the chronology of the ME PDCs (Liu and Wang, 1982; Liu et al., 1989, 1997; Liu and Xiang, 1997a,b; Cui et al., 1997, 2000; Yin et al., 2005, 2012; Xu et al., 2012; Oppenhimer et al., 2017), their stratigraphy (Yang et al., 1996, 2007; Liu, 2006; Wang et al., 2013, 2019; Zhao et al., 2013), geochemistry (Fan et al., 1999, 2006, 2007; Sui et al., 2007; Wei, 2010; Tang et al., 2014; Liu et al., 2015; Zhang et al., 2015; Chen et al., 2017; Pan et al., 2017a,b) and hazard (Wei et al., 1998, 2004b; Horn and Schmincke, 2000; Yu et al., 2013) since the 1980s. Previous investigations of the ME PDCs that focused on chronology and geochemistry found that the eruption occurred around 946 A.D, and indicated that there is a magma chamber at possibly 5–10 km depth below Tianchi volcano containing a mixture of rhyolites and trachytes (Machida and Arai, 1983; Liu, 1999; Fan et al., 2006, 2007; Wu et al., 2007; Wei, 2010; Xu et al., 2012; Kyong-Song et al., 2016; Chen et al., 2017; Oppenhimer et al., 2017; Pan et al., 2017a,b). However, relatively few stratigraphic studies have been conducted on the ME PDCs, and the ME facies model remains to be established.

To better understand emplacement processes, we investigate the PDCs emplaced during the ME in the Chinese territory

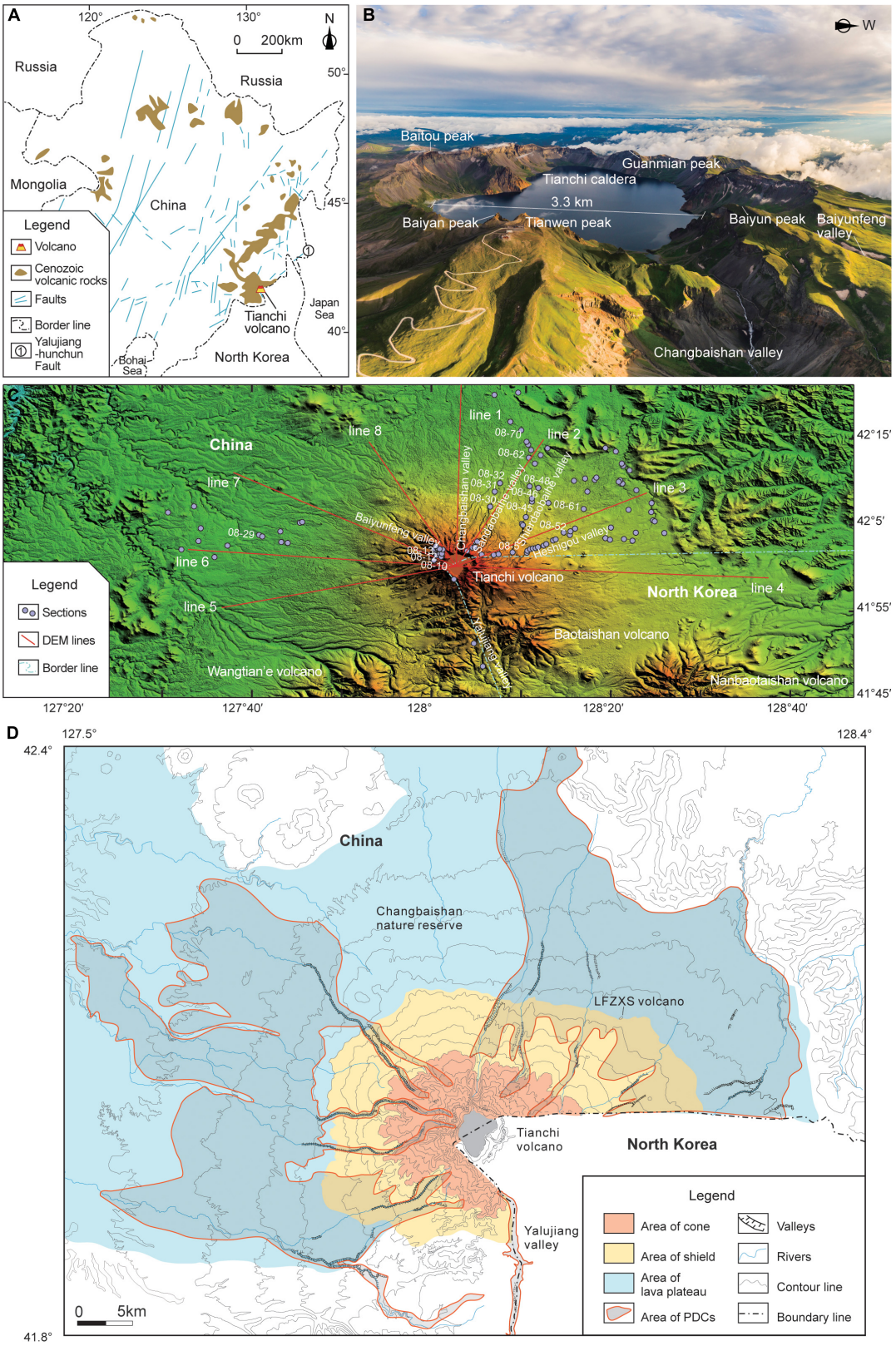

FIGURE 1 | (A) Location of Tianchi volcano, Cenozoic volcanic rocks and tectonic location in Northeast China (revised after Liu, 1999). **(B)** Aerial photograph of Tianchi caldera (photographed from north to south). **(C)** Digital elevation model (DEM) survey line and profile location of Tianchi volcano (DEM data from Alos30, Japan). **(D)** PDCs distribution of ME, and relationship with the area of the cone, the shield and the lava plateau (revised after Zhao et al., 2013).

via five aspects, i.e., the topography of Tianchi volcano, its stratigraphic, granulometric, and microscopic characteristics, and whole-rock composition, so as to establish the facies model of the PDCs during the ME.

MATERIALS AND METHODS

Topographic Analysis

The purpose of the DEM analysis was to study the characteristics of the PDC deposits emplaced during the ME in different landforms. Most of the primitive topography before the ME, including the lava plateau, shield and a part of the cone, has been preserved during the ME. Over the last 1000 years, the topographic changes have not been significant. Therefore, using the modern-day topography to analyze the PDC emplacement during the ME is still justifiable. The topographic data were obtained using Japan's Alos30 Digital Elevation Model (DEM) with a resolution of 30 m. The Global mapper was used with the Tianchi caldera as the center, to identify eight topography sections (**Figure 1C**) for the slope analysis of Tianchi volcano. This analysis was used to identify the Tianchi volcanic cone, lava shield, and lava plateau. The length of line 1, 2, 3, 4, 5, 6, 7, and 8 was 41, 30, 31, 45, 37, 41, 38, and 29 km, respectively.

Field Geological Survey

A geological field survey was conducted to collect samples and detail the stratigraphy of the PDC emplaced during the ME. Geological surveys, with a total of 104 working points and cross profiles, were performed along the Changbaishan, Shierdaobaihe, and Sandaobaihe valley on the northern slope, the Baiyunfeng valley on the western slope, and the Yalujiang valley on the southern slope near the cone and lava shield (**Figure 1C**; lacking data in North Korea's territory in the east). The purpose of focusing on the valleys was to ensure the continuity of the cross profile for a full comprehension of their attributes. Well-exposed outcrops on the lava plateaus were selected for mapping and sampling.

Granulometry

A grain size analysis was conducted on loose samples collected in the field. The measured grain diameter (d) ranged from 0.0625 to 64 mm (0.0625, 0.125, 0.25, 0.5, 1, 2, 4, 8, 16, 32 and 64 mm) and included 11 size grades from 4 to −6 phi (φ) (where $\varphi = -\log_2 d$, 4, 3, 2, 1, 0, −1, −2, −3, −4, −5, −6, respectively). The weight of the samples was typically 500 g, and a vibrating screen was used for screening. Inman (1952) has put forward the concepts of median diameter (Md_φ), which indicates the central size tendency and graphical standard deviation (σ_φ), which is a measure of sorting. The relevant formulae are: $Md_\varphi = \varphi_{50}$; $\sigma_\varphi = (\varphi_{84}-\varphi_{16})/2$, where φ_{50}, φ_{84} and φ_{16}, respectively represent the grain size of 50, 84, and 16% cumulative weight percentage, respectively.

The weight percentage of each grain size was measured, a histogram established, and the median phi value (M_φ) and graphical standard deviation (σ_φ) obtained. This method was used to compare the grain sizes of the samples collected at different locations to examine changes in the flow direction and transport mechanisms of the PDCs.

Microanalysis

The morphological characteristics of the PDC deposits were investigated at the microscopic level using microanalysis. This study used rock slice identification to examine the microstructure of the strongly welded rocks and large-particle pumices, and scanning electron microscope (SEM) to examine the surface characteristics of the small particle pumices. Microscopic analysis was used to identify the dynamic processes of the pyroclasts. A Carl Zeiss Axioskop 40 Polarizing Microscope was used to observe thin sections (magnification ranging from X5 to X150) in the CEA Key Laboratory of Seismic and Volcanic Hazards, Institute of Geology, CEA. Samples were analyzed using JEOL JSM-5610LV scanning electron microscope (SEM) in the SEM Laboratory of the Institute of Geology, Chinese Academy of Geological Sciences. The operation parameters included a 15 kV acceleration voltage, 10 μA electron current, and a magnification ranging from X100 to X2000. The SEM was operated between 15 and 25°C.

Whole-Rock Analysis

A whole-rock analysis was conducted to understand the geochemical composition of the pumices in the PDCs. Black and gray-white pumices were selected. The samples were tested in the laboratory of the Institute of Regional Geology and Mineral Resource Investigation in Hebei province, China. The instruments included an Axios^{max} X-ray fluorescence spectrometer, a P124S Electronic analytical balance, and Burettes. The analyses were conducted between 18 and 27°C.

Estimation of PDC Volume (V) in the Chinese Territory During the ME

The results of the topographic analysis and geological field survey around Tianchi volcano were based on the distribution of the PDCs. The PDCs were divided into four parts that include the plateau, shield, cone, and Yalujiang valley (**Figure 1D**). The area (A) and average thickness (AT) were calculated using the following equations:

(1) $V_{plateau} = A_{plateau} * AT_{plateau}$,
(2) $V_{shield} = A_{shield} * AT_{shield}$,
(3) $V_{cone} = A_{cone} * AT_{cone}$,
(4) $V_{Yalujiang} = A_{Yalujiang} * AT_{Yalujiang}$, and
(5) $V_{total} = V_{plateau} + V_{shield} + V_{cone} + V_{Yalujiang}$.

The above-mentioned formulas were used to calculate the PDCs volume during the ME in the Chinese territory.

RESULTS

Geomorphological Characteristics of Tianchi Volcano

The characteristics of the PDC deposits during the ME are closely related to the original geomorphology of Tianchi volcano. This

section explores the topography of Tianchi volcano and PDC deposits in different landforms.

Slope Characteristics of the Cone, the Lava Shield, and the Lava Plateau

The cone, lava shield, and lava plateau differ in slope because of different causes of formation. This study distinguishes between these three using the slope difference.

At least four eruptions occurred in the cone-forming stage of Tianchi volcano (Liu, 2000; Fan et al., 2006; Wei, 2014) and formed composite cones. The terrain of the cone fluctuates significantly, with a gentle slope at the bottom of the cone, reaching 30° near the caldera, and an average slope generally greater than 6° (**Figure 2**). The altitude of the cone base is above 1500 m, which is consistent with Luan (2008) and has an average distance of less than 10 km from the caldera.

The lava shield terrain is less undulating, with an average slope of 2–5° and an altitude of 1000–1500 m (**Figure 2**). The average distance between the lava shield and the center of the caldera is 10–20 km, while outliers reach 25 km.

The lava plateau has a gentle terrain, with the distance to the center of the caldera that is typically greater than 20 km, an average slope less than 1°, and an altitude typically less than 1000 m (**Figure 2**).

Distribution of the PDCs on the Cone, Lava Shield, and Lava Plateau

The gully-type deposits on the cone are within 0–10 km from the center of the caldera. Furthermore, the deposits are mainly distributed in radial canyons near the cones, such as the Changbaishan, Sandaobaihe, and Shierdaobaihe valley on the northern slope, the Baiyunfeng valley on the western slope, and the Yalujiang valley on the southern slope (**Figure 1C**). PDC deposits were observed in the upper reaches of the Shiderdaobaihe valley (**Figure 3A**) and have a thickness between 1 and 4 m (**Figure 4**), whereas massive continuous PDC deposits were rarely observed on the surrounding mountain slopes.

Valley-type deposits on the volcanic shield are 10–20 km away from the center of the caldera. Furthermore, PDCs that were deposited in the valleys of the lava shield have an exposed

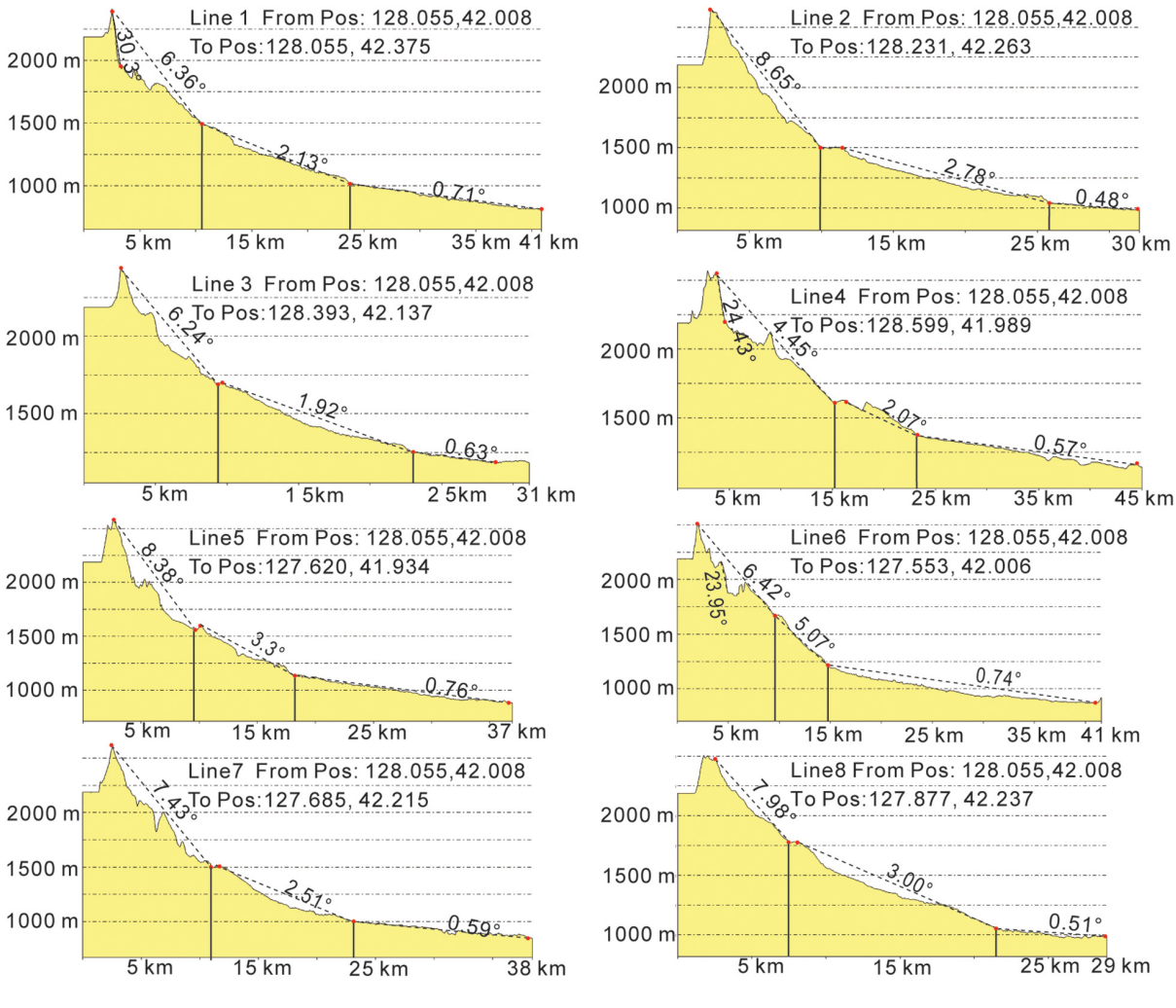

FIGURE 2 | Digital Elevation Model profile of the Alos30 image of the Tianchi volcanic cone, lava shield, lava plateau, and slopes (from line 1 to line 8).

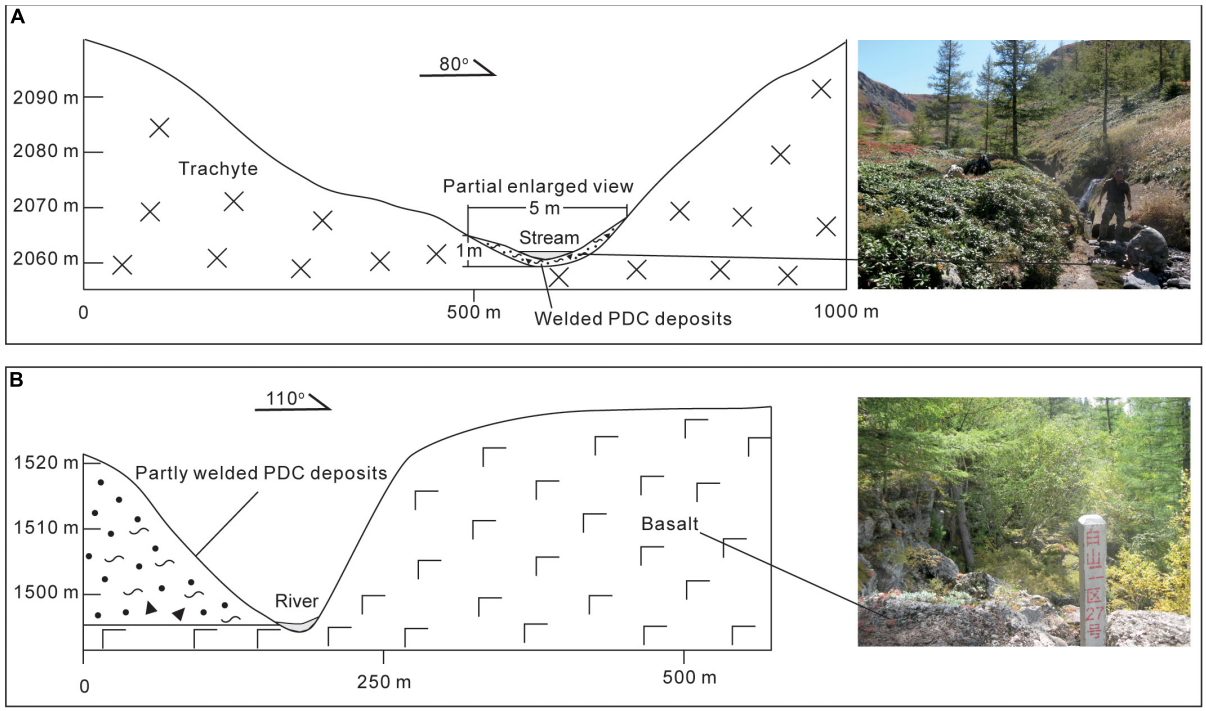

FIGURE 3 | (A) Schematic of the Shierdaobaihe gully-type deposits. **(B)** Schematic of Shierdaobaihe basalt valley deposits.

thickness between 10 and 20 m (**Figure 4**), whereas no massive PDC deposits were found on the basalt shield, at the top of the cliff (**Figure 3B**).

The lava plateaus constitute an area of open terrain and gentle slope. Fan-shaped deposits on the lava plateau are more than 20 km away from the center of the caldera, including two large fan-shaped deposits on the northeast and west sides. PDC deposits are typically less than 10 m thick in the exposed low land or river profiles (**Figure 4**).

The existence of volcanoes such as Wangtian'e and Baotaishan (**Figure 1C**) causes the landform in the southern part of Tianchi volcano to be more uneven than those in the northern and western slope, featuring numerous canyons. Influenced by the original terrain of the volcanoes on the southern slope, the PDC in the Yalujiang valley has valley branch-type deposits that have a maximum exposed thickness of 60 m.

In summary, PDC deposits are controlled by the original topography of Tianchi volcano. The thickest deposits were found in the lava shield, and thin deposits were found in the cones and lava plateaus. The PDCs rushed out of the canyon channel to form fan-shaped deposits in the lava plateau. The distribution of the PDCs during the ME shows that the PDC deposits radiate outwards from the center caldera, the periphery has a pyroclastic apron with at least two fan-shaped deposits, and the branch-type valley deposits are joined in a near-circular shape.

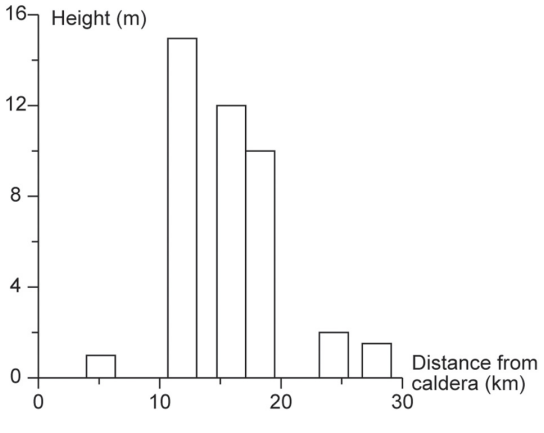

FIGURE 4 | Distribution of stratum thickness in the Shierdaobaihe valley.

Stratigraphic Characteristics of the PDCs in the ME

The preliminary analysis is divided according to the characteristics of the volcanic topography, PDC distribution patterns, and the PDC strata. Therefore, the ME PDC deposits were divided into three types: proximal deposits in the cone (0–10 km), medial deposits in the shield (10–20 km), and distal deposits in the lava plateau (> 20 km). This profile explores the structures of the proximal, medial, and distal PDC deposits.

Characteristics of the Proximal Strata

Proximal ME PDC deposits cover the peaks around the Tianchi caldera, parts of the mountain slopes that surround the cone, and the valleys.

(1) Stratigraphic characteristics of ME deposits in Tianchi volcano peaks

Fallout and spatter deposits are exposed at the different Tianchi volcano peaks. The stratigraphic characteristics of the Tianwen Peak and Baiyan peak on the northern slope, Baiyun Peak on the western slope, and Guanmian Peak on the southern slope are examined.

Tianwen Peak and Baiyan Peak are on the north side of the Tianchi caldera. Pumice strata can be seen at the Tianwen Peak, with colors from bottom to top ranging from gray, yellow, gray-white, to black (**Figure 5A**). Among them, gray and yellow pumices are considered to be eruptive products from 5,000 years ago (Liu et al., 1998; Yu et al., 2012). The gray-white pumices are ME rhyolites with a thickness of 10–20 m (Liu et al., 1998; Liu, 2000; Fan et al., 2005; Wei et al., 2007; Yu et al., 2012). The black trachyte pumices are considered to be the product of the 1702 eruption (**Figure 5B**; Liu et al., 1996; Liu, 2000; Wei et al., 2007). Baiyanfeng has a similar stratigraphic sequence (**Figures 5C,D**).

Fan-shaped gray-white pumice deposits, with an exposed thickness of 2–4 m exist on the outer slope of the Baiyun Peak which is located on the west side of Tianchi volcano (**Figure 5E**). The fan-shaped deposits are surrounded by alpine meadows, and the gray-black ME deposits can be seen in the gullies on the edge of the meadows (**Figure 5F**).

Fallout ME pumice strata are observed at the Guanmian Peak with a gentle slope on the south side of Tianchi volcano and the outer sections (**Figure 5G**), which covered larger areas than that on the northern and western slope. The thickness of the exposed formation is 0.5–2 m. The primary composition of the formation consisted of gray-white pumices and a small amount of gray-black trachyte lithic (**Figure 5H**).

(2) Stratigraphic characteristics of the ME PDCs in the gullies near the Tianchi cone

The gullies that are within 10 km from the center of the Tianchi caldera and have ME PDC thicknesses between 1 and 4 m consist of three types of structures (i.e., eutaxitic and lava-like structures). Large-scale continuous PDC deposits rarely occur on the mountain slope surrounding the cone.

The PDC deposits are distributed in the stream gully at the bottom of the Shierdaobaihe valley on the northern slope of Tianchi volcano (profile point 08-5 on the Chinese-North Korean border, 42.029829°, 128.125317°). The PDC deposits are approximately 5.1 km away from the center of Tianchi volcano and extend roughly 1 km northward into China. However, this is not the case in North Korea. The stratum is typically 1–2 m thick and appears to be mostly gray, with a high degree of welding and eutaxitic structures (**Figures 6A,B**). The eutaxitic structures are mainly composed of gray, gray-black magma fragments, and brick-red lithic fragments. The magma fragments are stretched and directional (**Figure 6B**).

Profile 08-10 (42.013284°, 128.015645°) is located at Baiyunfeng valley on the western slope of Tianchi volcano and is 3.38 km away from the center of Tianchi volcano. The ME deposits have an uneven thickness and extend steadily along the gully. The stratum has lag breccias (**Figure 6C**) formed during the ME. Profile 08-10 is completely gray-black, has an exposed thickness of 3–4 m, has high volumes of lag breccias, a semi-angular shape, a particle-supporting structure, a typical grain size of 60 cm, and maximum values reaching 1 m.

Profile 08-12 is located 100 m west of profile 08-10 and display different stratigraphic characteristics. The formation is completely gray-black and has a thickness between 4 and 5 m (**Figure 6D**). The stratum is divided into three parts. The upper part is 2–3 m thick and comprises welded tuffs containing breccias. The middle part is approximately 1 m thick and has parallel beddings with plastic flow characteristics (**Figure 6E**). There are bends in certain locations that were possibly caused by the secondary flow of fragmented magma falling to the ground, which serves as high temperature near the caldera. Under the parallel beddings there is a gray-black pumice-rich layer with bombs that have a gray-white fresh surface which is uncovered when smashed with a hammer (**Figure 6F**). The lower part consists of gray-black breccia tuffs that have a thickness of 1–2 m.

Profile 08-13 is located 30 m west of profile 08-12, without the intermediate bedding of profile 08-12 (**Figure 6G**). A stalactite-like structure has been found in the pumice-rich layer cavity (**Figure 6H**). The Stalactite-like structure hangs upside down, with a thick feature on the top and a thin feature on the bottom. The surface is rough. This is similar to stalactite. It is not common in the proximal deposits. Compared with lava stalactites (Corsaro et al., 2005), the structure has a rough surface, does not originate from the lava flow, and is probably related to volcanic ash dribbling in the cavity.

Characteristics of the Medial Strata

In the canyons 10–20 km away from the center of the Tianchi caldera, the medial strata generally have thick-bed deposits, irregular columnar joints, lithic-rich layers, pumice-rich layers, and welded layers.

(1) Columnar joints

Columnar joints developed in the Sandaobiahe valley on the northern slope of Tianchi volcano. Profile 08-31 (42.137471°, 128.128201°) is 15.5 km from the center of Tianchi volcano and is a PDC river island formed as a result of river incision (exposed thickness of 4–5 m). The Sandaobaihe River runs along the west edge of the river island (**Figure 7D**). On the eastern edge of the river island (**Figure 7E**) the river channel has dried up. Columnar joints developed on both sides of the river island and have a strong degree of welding and weakening on both sides. Profile 08-30 shows that the river flows through the fissures or columnar joints formed during medial PDC cooling, thereby forming a river channel. Profile 08-32 (**Figure 7C**) is 500 m north of profile 08-31 and has an overall thickness between 8 and 10 m. The top layer consists of gray-yellow tephra. The middle part has irregular columnar joints, and the lower part has a groove that has been eroded by rivers. The columnar joints are narrower in the upper part and wider in the middle and lower parts. The degree of welding weakens from the middle to the upper and lower sides.

Profile 08-30 (42.125156°, 128.118694°) is located approximately 14 km away from the center of Tianchi

FIGURE 5 | Tianchi volcano peaks and strata. **(A)** Tianwen Peak on the northern slope. **(B)** White and black pumice at Tianwen Peak. **(C)** Baiyan Peak on the northern slope. **(D)** Stratigraphic profile of Baiyan Peak. **(E)** Gray-white pumice on the outer slope of Baiyun Peak. **(F)** welded agglomerate at the outer slope of Baiyun Peak. **(G)** Guanmian Peak on the southern slope. **(H)** pumice deposits at Guanmian Peak on the southern slope.

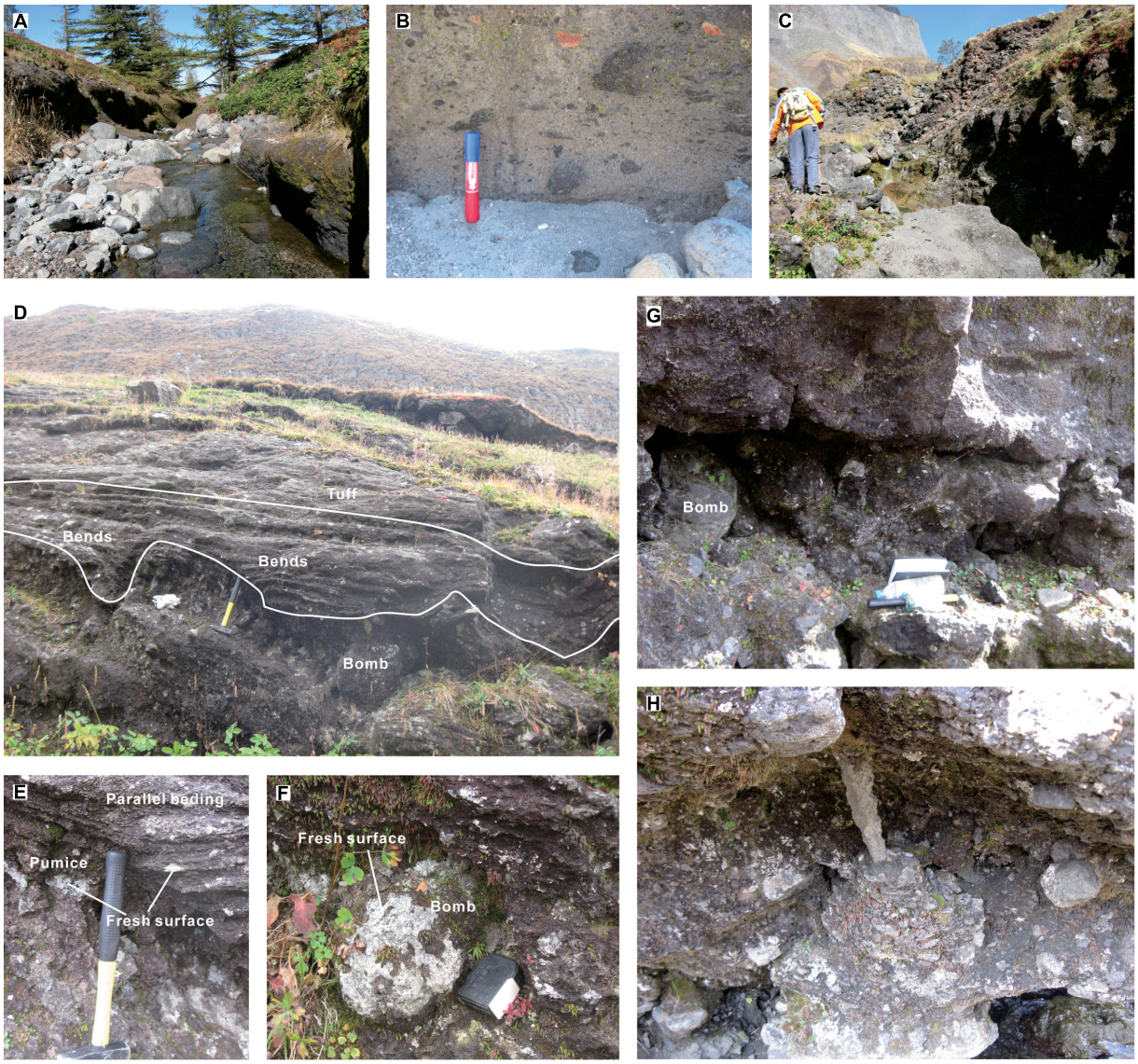

FIGURE 6 | (A) Deposits in the gullies of Shierdaobaihe valley. **(B)** PDC eutaxitic structures. **(C)** Profile 08-10 of Baiyunfeng valley. **(D)** profile 08-12 and plastic layers of Baiyunfeng valley. **(E)** Parallel bedding of profile 08-12. **(F)** Bombs in the profile 08-12. **(G)** Profile 08-13 of Baiyunfeng valley. **(H)** 08-13 stalactite-like structure.

volcano in the Sandaobaihe valley and has block structures with irregular shapes and different sizes, typically ranging from 0.4 to 1 m (**Figure 7A**). In the tracing process, we found that the block structures were formed through collapsed and strongly welded strata (i.e., columnar joints) because of the subsequent impact of the river and weathering (**Figure 7B**). The block structures are secondary features of the ME PDCs.

(2) Lithic-rich layers, pumice-rich layers, and welded layers

Profile 08-52 of Heishigou valley (42.058599°, 128.257290°) is located on the northern slope of Tianchi volcano and is 16.7 km away from the center of the caldera. The bottom of the PDCs is rich in lithic (**Figure 8A**). This formation is 30–40 cm thick, has no welding, and is supported by the tephra matrix. This formation has a massive amount of basalt and trachyte lithics. The grain size of a few lithics reaches 30 cm, and the long axis of the lithics typically points to one direction.

Profile 08-45 (42.134839°, 128.2°) of the Shierdaobaihe valley is located on the northern slope of Tianchi volcano and is 18.5 km away from the caldera. The formation is approximately 15 m thick. A lenticular pumice-rich layer (**Figure 8B**) was found at the base with a thickness of approximately 2 m. The lens contains gray-black pumice and a little black ash that was probably obtained from the top deposits. The size of pumice is typically between 6 and 8 cm, with the largest particles reaching approximately 12 cm. Profile 08-46 is located 200 m north of

FIGURE 7 | (A) Block tuff structures in profile 08-30. **(B)** Irregular columnar joints and block tuff structures at the top of profile 08-30. **(C)** Irregular columnar joints in profile 08-32. **(D)** Columnar joints at the west edge of the River Island in profile 08-31. **(E)** Columnar joints at the east edge of the River Island in profile 08-31.

profile 08-45 and shows different stratigraphic characteristics. The stratum developed at least five welded layers (**Figure 8C**) that are common in the Yalujiang valley.

Profile 08-48 (42.16922°, 128.189882°) of Shierdaobaihe valley is located on the northern slope of Tianchi volcano and is 19.6 km away from the caldera. The compacted formation is completely gray-black. A long-strip pumice-rich layer (**Figure 8D**) exists in the middle of the profile and has an uneven thickness distribution of 0.5–1 m.

In summary, the stratigraphic structure of the medial PDC deposits has the following characteristics. (a) Columnar joints in the middle and upper reaches of the medial PDCs. The formation in the lower reaches of the medial PDCs has no welding. The degree of PDC welding decreases with distance from the caldera. (b) The development of lithic-rich layers and pumice-rich layers shows a gravitational differentiation effect.

Characteristics of the Distal Strata

The distal strata of the lava plateau mainly consist of loose deposits of gray and gray-white pumices. The stratigraphic structures mainly include climbing layers, coarse-tail layers, and ground surge layers. Additionally, reworked pyroclastic deposits occur in this area.

Profile 08-61 (42.111016°, 128.218616°) is located on the northern slope of Tianchi volcano and is 17.48 km from the center of the caldera. The PDCs cover the slope of Laofangzixiaoshan (LFZXS) volcano and form a climbing layer (**Figure 9A**). Profile 08-61 is ash cloud surge deposits supported

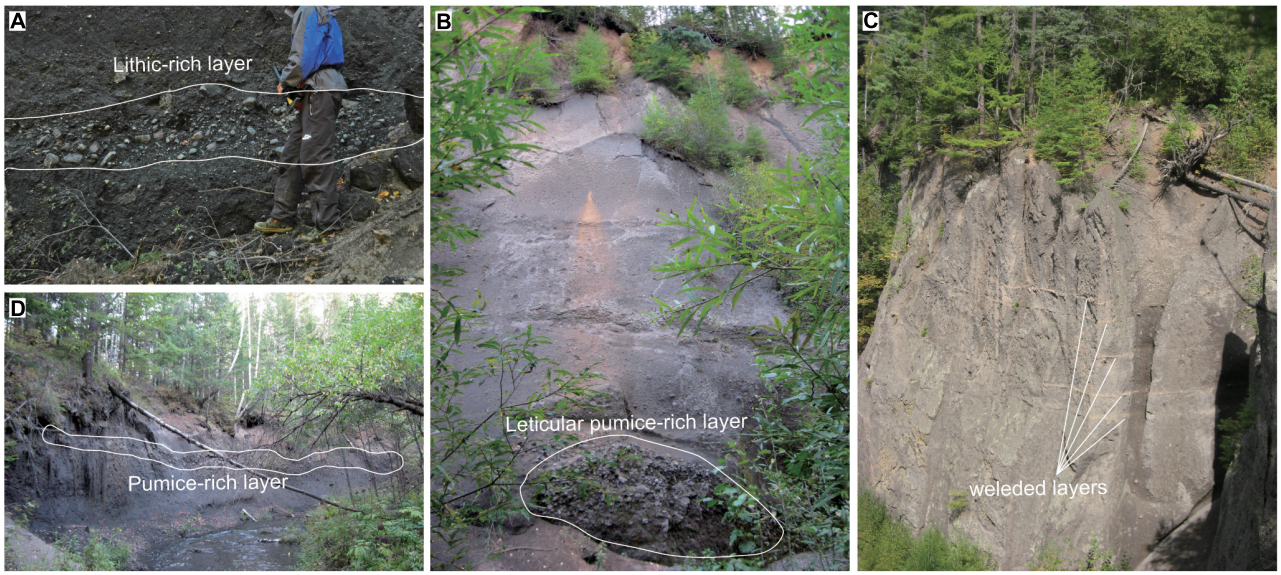

FIGURE 8 | (A) Profile 08-52 of lithic-rich layers. **(B)** Profile 08-45 of lenticular pumice-rich layers. **(C)** Profile 08-46 of welded layers. **(D)** Profile 08-48 of long-strip pumice-rich layers.

by a tephra matrix. The grain size is well sorted. Coarse-grained pumices are partially exposed, and have a size of approximately 3–4 cm. The stratum under the ash cloud is composed of brick red spatter deposits of LFZXS volcano. A definite boundary exists between the gray ash cloud layer and the ejected stratum of LFZXS volcano. The ash cloud climbed over LFZXS volcano.

Profile 08-62 (42.189783°, 128.227088°) is located on the northern slope of Tianchi volcano and is 24.8 km from the center of the caldera. Profile 08-62 has a typical coarse-tail layer (**Figure 9B**) with an exposed thickness of approximately 2 m. Profile 08-62 is completely supported by a gray-white matrix of ash that is roughly divided into 4 layers, from top to bottom. The first layer is rich in large-particle pumices and contains several plant roots. The size of the lithic is typically 6–8 cm in the upper part and gradually decreases to a grain size of 2–4 cm in the lower part. This shows the characteristics of a reverse graded bedding, with relatively concentrated coarse-grained pumices. The second layer consists of tephra deposits with a gas escape structure. The third layer consists of pumice deposits supported by the tephra matrix, which have typical pumice sizes of 2–4 cm. The fourth layer consists of tephra and contains a small amount of large-particle pumices, which have a larger grain size of approximately 3 cm.

Profile 08-29 (42.054684°, 127.659861°) of the distal PDCs is located to the west of Tianchi volcano, is approximately 33 km away from the center of the caldera, and shows cross and diagonal bedding (**Figure 9C**). The lower part is a layer rich in coarse-grained pumices with a thickness of approximately 50 cm and a long axis of 6–8 cm in length. Loose tephra is filled between the pumice layers.

Profile 08-70 (42.262282°, 128.168213°) is located on the northern slope of Tianchi volcano, is approximately 30 km from the center of the caldera and is a reworked pyroclastic layer. Profile 08-70 is similar to the base-surge stratum and has a parallel bedding and pumice-rich layer (**Figure 9D**). The pumice-rich layer has a granular structure, contains no ash, and has a high degree of roundness. The bottom of the pumice-rich layer contains a 0.5 cm thick yellow-brown soil layer, which extends smoothly. The lower part of the soil layer is the original PDC stratum.

Additionally, carbonized wood is common in the distal part. The largest outcrop of carbonized wood in the PDCs is on the southern slope, which has become a scenic spot for tourists to visit (**Figure 9E**).

In summary, the deposits in the distal strata are lighter in color (gray-white) and have loose deposits.

Granulometry

The grain-size distribution is essential when characterizing PDCs. In this study, the comparison of stratigraphic profiles, medial values, and histograms of the medial and distal PDCs of the Shierdaobaihe valley was established to investigate the variation in grain size and clastic composition. The strata analysis covered most of the PDC deposits, such as ash cloud, ground surge, and pumice-rich layers.

The histograms of the main flow unit of the PDCs, except for the ash clouds and ground surges, show a multimodal distribution (**Figure 10**). The median phi size (Md_{φ}) is between −2.5 and 3.25, and the histogram shows a non-uniform distribution. The sorting coefficient (σ_{φ}) is typically greater than 2 and includes poor sorting that has a skew-normal data range between −1.15 and 1.48, but no apparent total skewness. The kurtosis is mostly less than 1.

The histograms of the ash cloud are characterized by a unimodal distribution (**Figure 10**). The median phi size (Md_{φ})

FIGURE 9 | (A) Profile 08-61 of climbing layers. **(B)** Profile 08-62 of coarse-tail layers. **(C)** Profile 08-29 of ground surge layers. **(D)** Profile 08-70 of reworked PDC strata. **(E)** Outcrop of carbonized woods in PDCs.

is typically greater than 3, which indicates a concentration approaching that of fine particles. The sorting coefficient (σ_φ) is typically less than 2 and has an overall good sorting despite the poor sorting of individual cases, which may be caused by large-particle pumices in the bottom layer. Skewness values ranging between −0.23 and 0.2 demonstrate an overall negatively skewed distribution approaching that of fine particles. Most kurtoses are greater than 1 and have a higher spread ratio than that of the main flow unit of PDCs.

The histogram distribution of the ground surge layers is similar to that of the ash cloud deposits (**Figure 10**). The median phi size (Md_φ) is greater than 3, and the sorting coefficient (σ_φ) is less than 2. An adequate overall sorting is observed with a skew-normal data range between −0.23–0.2 and an overall negatively skewed distribution slightly approaching that of fine particles. The kurtosis is greater than 1.

The histograms of the pumice-rich layers show two protruding ends and a receding center (**Figure 10**). The pumice-rich layers are characterized by a dominant percentage of coarse grains and relatively large amounts of volcanic ash, rather than small amounts of medium-sized particles.

Microscopic Morphological Analysis

Microstructure Analysis

(1) Microstructure analysis of proximal pyroclasts

The internal structure of the pumices of the ME at the Tianwen Peak on the northern slope of Tianchi volcano is characterized by vesicular structures. Some pumice vesicles are heavily elongated and appear as thin lines with a parallel orientation (**Figure 11A**). Some vesicles are less elongated and appear in a lenticular shape (**Figure 11B**). A mixed structure was also observed that macroscopically appears as gray-white pumices, containing black lumps and microscopically appears as black pumices blended into gray-white pumices (**Figure 11C**). The boundary between the black part and the surrounding light-colored part is unclear, probably because of magma mixing.

FIGURE 10 | Profile, vertical medial, and histogram variation of medial and distal PDCs of Tianchi volcano.

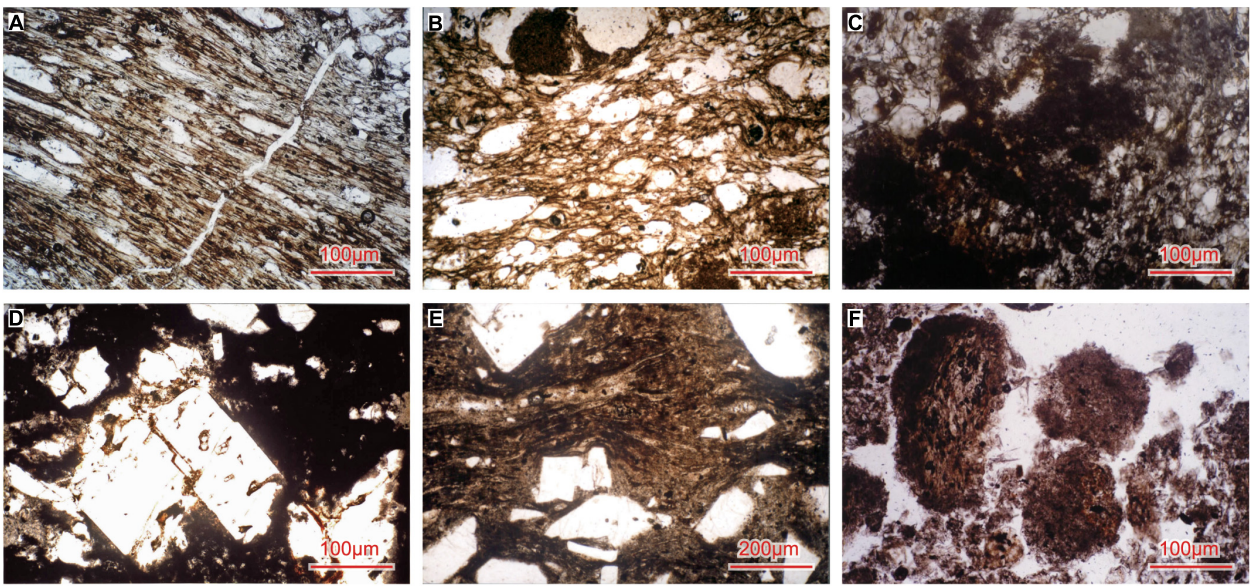

FIGURE 11 | (A) Stretched vesicular structure. **(B)** Lenticular-shaped stretched vesicular structure. **(C)** Welded structure of gray-white and black pumice. **(D)** Lava structure. **(E)** Tuffaceous structure. **(F)** Mud mass structure.

A sample of profile 08-5 of the ME PDC on the northern slope of Tianchi volcano shows breccia lava structures under a microscope (**Figure 11D**). This indicates that the proximal PDC deposits were partially formed by interstitial melt.

(2) Microstructure analysis of medial pyroclasts

Tuffaceous structures are typically developed in the medial strata (**Figure 11E**). The corrosion degree of crystal fragments is usually weak. The cementation consists of extremely fine ash, which is vitreous and different from lava cementation. This cementation is not as even as that of fast-cooling lava and demonstrates fibrous and needle-like vitreous forms under the microscope. The cementation of some samples shows curved directional strips.

(3) Microstructure analysis of distal pyroclasts

Mud masses are developed in the ash cloud layer of profile 08-61 on the northern slope of Tianchi volcano (**Figure 11F**). The strata appear to be earthy gray owing to the existence of mud masses (**Figure 9A**). Therefore, profile 08-61 has a different color from that of other distal profiles. Two reasons may account for the formation of mud masses: the first is *in situ* weathering, and the second is secondary transportation. The stratigraphic profiles indicate that the mud masses in profile 08-61 were formed as a result of *in situ* weathering.

Morphological Analysis

Samples for this ME morphological analysis were derived from profiles 08-45 and 08-62, 08-29, 08-70 of the PDCs, ground surge layers, and secondary pyroclastic strata, respectively. The SEM was used to observe the impact craters, cracks, and a large number of attachments on the surface of the PDC particles.

A "petal-shaped" impact crater was observed on the particle surface of the PDC profile 08-62 (**Figure 12A**). The fragmentation caused by the impact on the original surface has sunken into the interior of the particles, with appendages in the center and radial cracks spreading outwards. As the impact intensified, the fragments fell off and formed a near-circular impact crater (**Figure 12B**).

Fracture textures that formed as a result of quenching were observed on the clastic surface of the PDC and ground surge profiles. Cracks in the PDCs have a "linear" or "Y" shape (**Figure 12C**). Cracks in the ground surge layers resemble turtle shells (**Figure 12D**), consisting of a smooth surface, which turns outwards and almost covers the entire clast surface. Different shapes of cracks suggest an increasing quenching effect, which starts from "linear" to "Y" and progresses to a "turtle shell."

Volcanic ash in the PDCs has sharp edges, sharp corners, and numerous small particles attached to the surface (**Figure 12E**). The reworked ash is sub-angular in shape, and some samples appear rounded, with a few appendages on their relatively clean surface (**Figure 12F**).

Whole-Rock Analysis

A whole-rock analysis was used in to examine the composition of the black and gray-black pumices (magma fragment samples) from the proximal and medial strata and the gray-white pumice samples from the distal strata.

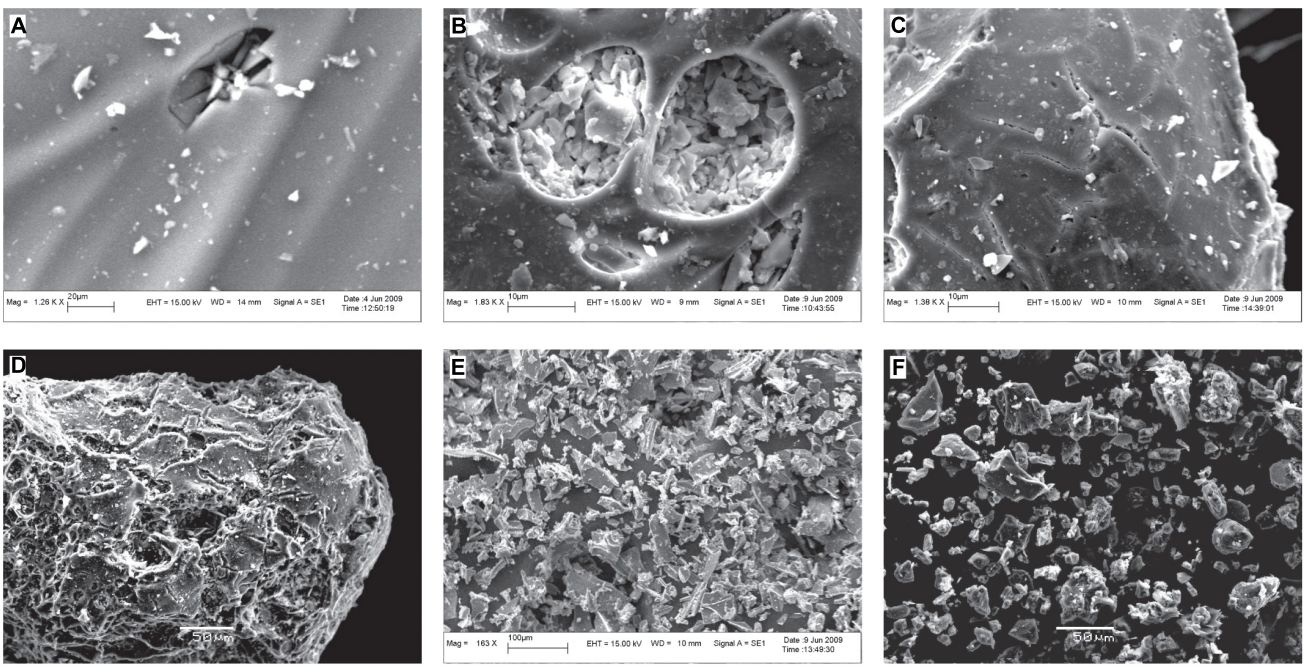

FIGURE 12 | (A) "Petal-shaped" impact crater. **(B)** Circular impact craters and appendages. **(C)** "Linear"- and "Y"-shaped cracks. **(D)** "Turtle shell" crack structure. **(E)** Ash morphology of PDCs. **(F)** Ash morphology of reworked deposits.

The total alkali-silica (TAS) diagram shows that the components of the gray-black pumice (magma fragment strips in the gray white pumice) at points 08-5, 08-45, and 08-52 in the Shierdaobaihe valley are projected in the trachyte zone. However, the components of the distal strata 08-29, 08-60, and 08-62 are projected in the pantellerite zone (**Figure 13** and **Table 1**). Shi et al. (2005) suggested that the white pumices that erupted during the ME are rhyolitic, and the black pumices are trachytic. Fan et al. (2005) proposed that the gray-black and gray-white ME pumices are the ejected products of the trachytic basaltic magma. The results of the TAS diagram in this study and the ME samples of Fan et al. (2005) and Shi et al. (2005) correspond well.

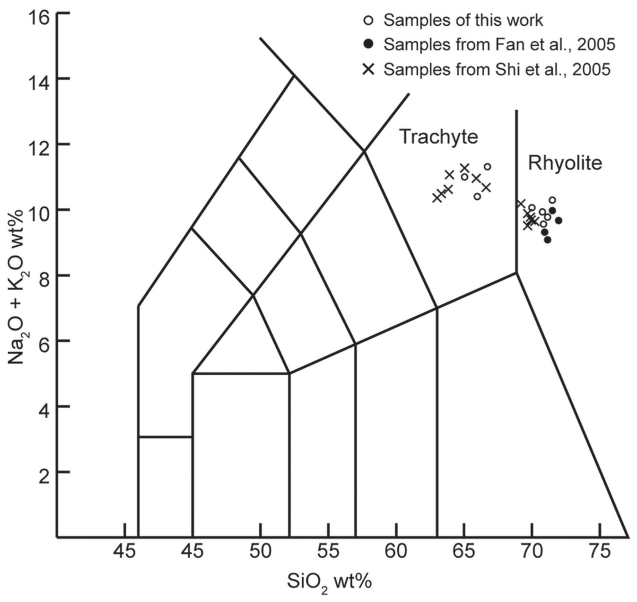

FIGURE 13 | Total alkali-silica diagram of pyroclastic rocks from the ME of Tianchi Volcano (Le Maitre, 1989).

TABLE 1 | Datasheet of the whole-rock test.

Major element	08-5	08-29	08-45	08-52	08-60	08-62
SiO_2	66.46	69.88	65.86	64.86	71	70.6
Al_2O_3	14.96	11.28	13.67	14.28	10.94	11.28
TiO_2	0.36	0.29	0.36	0.34	0.24	0.3
Fe_2O_3	2.11	1.91	2.37	2.29	1.81	2.06
FeO	2.37	2.71	2.68	2.73	2.56	2.63
CaO	1.04	0.77	1.23	1.12	0.5	0.58
MgO	0.19	0.15	0.19	0.18	0.11	0.14
K_2O	5.52	4.64	5.37	5.33	4.49	4.56
Na_2O	5.73	5.36	5.01	5.63	5.23	5.32
MnO	0.126	0.096	0.123	0.13	0.089	0.091
P_2O_5	0.06	0.09	0.08	0.11	0.06	0.07
H_2O^+	0.25	1.92	2.52	2.12	2.08	1.78
H_2O^-	0.25	0.36	0.45	0.18	0.34	0.28
Loss	0.4	2.65	2.92	2.52	2.65	2.38
Total	99.33	99.83	99.86	99.52	99.68	100.01

Volume Estimation

The PDCs deposited during the ME contain two fan-shaped and valley deposits in the Yalujiang valley. The PDC areas were divided into four parts, including the plateau, shield, cone, and Yalujiang valley. The area and average thickness of these four parts were calculated and are listed in **Table 2**. The estimated volume of PDCs deposits in the Chinese territory during the ME was calculated to be approximately 7 km^3.

DISCUSSION

The volume of the PDCs in the Chinese territory is estimated at approximately 7 km^3. This value is close to the result of 8.5 km^3 from Liu and Xiang (1997a), but it is smaller than the result of 19.2 ± 2.6 km^3 from Horn and Schmincke (2000). The difference between this work and Horn and Schmincke results is probably due to two factors. Firstly, according to Horn and Schmincke (2000), the volume estimate probably included the PDC and proximal tephra deposits in North Korea. Secondly, Horn and Schmincke (2000) reported that the PDC covered a half area to the north around the caldera. However, according to our field work, the distribution of PDC is just like a fan shape in the north, which is smaller. The volume estimations of fallout tephra during ME vary from 83 to 120 km^3 (Liu and Xiang, 1997a; Horn and Schmincke, 2000; Yu et al., 2012). Although a big difference in the tephra volume estimations exists, it is widely accepted that the total volume is about 100 km^3 (Wei, 2010; Yu et al., 2012; Pan et al., 2017a). The 1991 eruption of the Pinatubo volcano produced 3.3–4.4 km^3 tephra and was ranked among the five largest eruptions of the 20th century (Paladio-Melosantos et al., 1996). The 2010 eruption of the Merapi volcano produced 0.04 km^3 of PDC deposits and reached a distance of 16 km from the crater (Bignami et al., 2013). Therefore, the scale of the ME is much larger than that of these eruptive events.

The distribution of the PDCs during the ME shows that the palaeotopography influenced the emplacement of the PDCs (i.e., valley-filled deposits). Valley-filled PDC emplacements are common and have also been observed in the 2007 Soufrière volcano eruption (Wadge et al., 2014) and the 2010 Merapi volcano eruption (Bignami et al., 2013). Branney and Kokelaar (2002) proposed that PDCs from a large-volume eruption are minimally affected by the original surface topography, such as the Matahina ignimbrite volume of 120 km^3 of the Taupo volcanic zone (Bailey and Carr, 1994). The volume of the PDCs during the ME is approximately 7 km^3 in the Chinese territory, far less than the volume of the Matahina ignimbrite. Therefore, when considering volume, the PDC emplacement during ME did not get rid of the influence of the original

TABLE 2 | Parameters of the plateau, shield, cone, and Yalujiang valley.

Location	Plateau	Shield	Cone	Yalujiang valley	Total
A (km^2)	1366	152.5	45.8	8.4	1572.7
AT (km)	0.003	0.014	0.002	0.06	
V (km^3)	4.098	2.135	0.0916	0.504	6.9806

topography. The stratigraphic evidence shows that the ash cloud during the ME climbed over LFZXS volcano (**Figure 1D**). Ash clouds are turbulent, represent low-density flows, and can move independently (Cas and Wright, 1987). The unimodal distribution of the histogram shows a single transportation process of ash cloud deposits that was primarily in the form of a suspended transportation. The suspended transport of ash clouds floated over the LFZXS volcano and a part of it emplaced on the hill during the ME.

Temperature is an important physical parameter for PDCs. Blong (1996) proposed that the PDC temperature ranged from 100 to 900°C. The stratigraphic evidence shows that carbonized woods developed in the distal deposits during the ME. The carbonization temperature of wood is above 280°C. Columnar joints were discovered in the medial strata. Through the remanent magnetization analyses of lithic clasts, Wright et al. (2011) estimated the Cerro Galán PDC formation temperature of columnar joints to be above 630°C but below the glass transition temperature. Plastic behavior occurred in the proximal deposits. Zou et al. (2010) reported that the rhyolite magma of Tianchi volcano has a temperature of 740 ± 40°C. Therefore, the temperature of the PDCs during the ME probably ranged between 280 and 740°C, from the distal to the proximal deposits, respectively. In the 1997 Soufrière volcano eruption, the dilute and slow PDCs did not have enough kinetic energy to destroy the weaken buildings (Loughlin et al., 2002). However, the hot ash (> 300–400°C) set off the fire in the buildings and caused lethal burns on direct contact with the skin (Baxter et al., 2005). The same happened again in the 2010 eruption of Merapi volcano. People in the buildings did not survive in the relatively low temperature PDCs (250–300°C), partly because of the hot ash, floating into the buildings' interior through the vent (Jenkins et al., 2013). The run-out distances of PDCs in these two historical eruptive events did not exceeded 16 km (Loughlin et al., 2002; Jenkins et al., 2013). Temperatures above 280°C were maintained beyond 20 km from the Tianchi caldera; thus, the destruction potential of the PDCs associated with the ME must have been remarkable.

The fallout tephra and spatter deposits from the ME remained at the Tianchi Peaks in Chinese borders and have a relatively low thicknesses, which is probably due to three factors. Firstly,

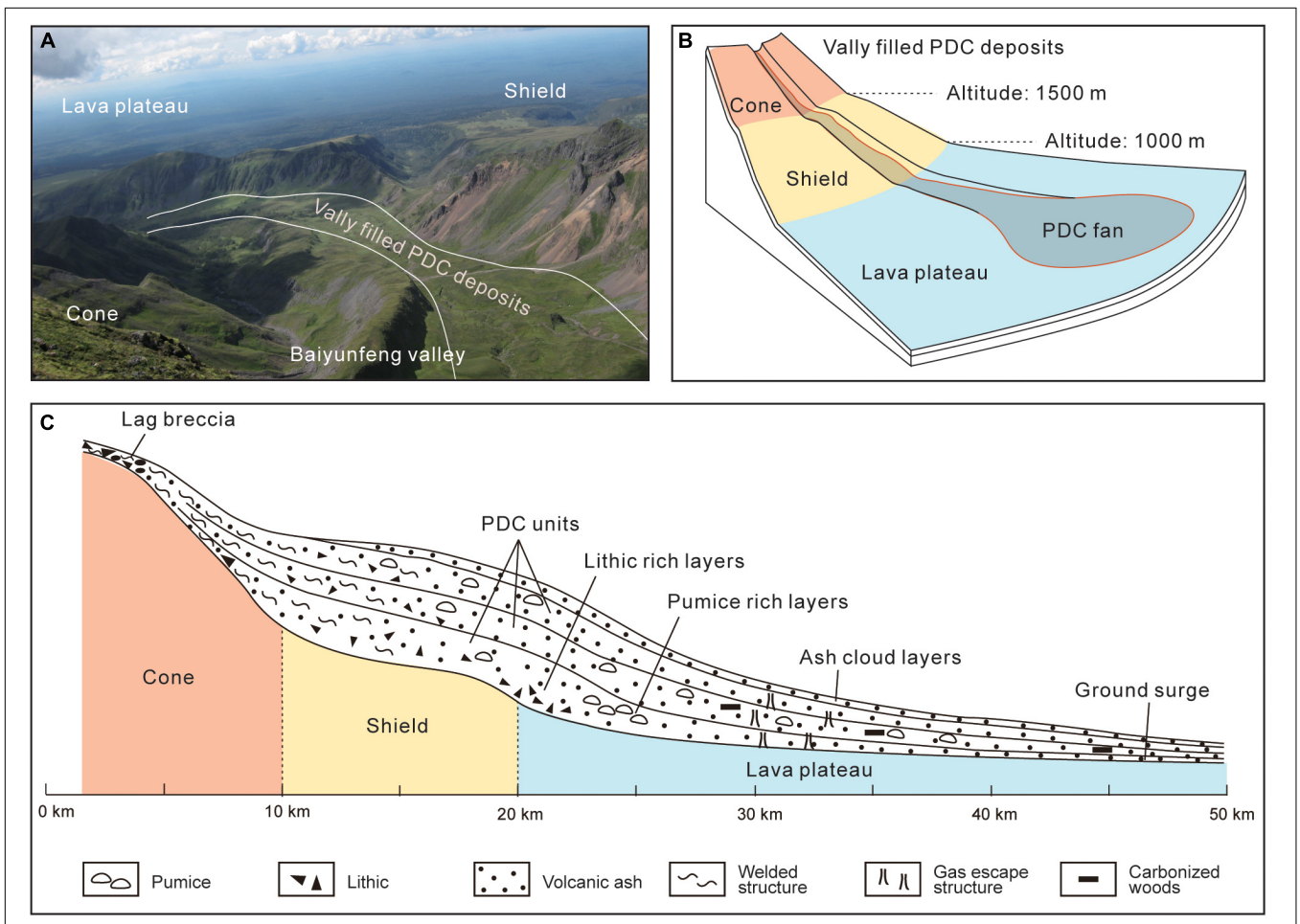

FIGURE 14 | (A) Picture of Baiyunfeng valley. **(B)** Schematic of the PDCs deposition in different terrains of Tianchi volcano. **(C)** PDC facies model of the ME of Tianchi volcano.

the wind was primarily directed toward the east, with a season-dependent intensity (Yu et al., 2013). Fallout tephra heavily accumulated in North Korea because of the wind direction. Secondly, the inclined eruption column could result in an uneven thickness. Thirdly, numerous eruptions occurred, where later eruptions eroded the material and mountain peaks of the earlier ones.

The black pumice at Tianwen Peak was supposed to be the product of the 1702 eruption (Liu et al., 1996). However, Pan et al. (2017a) proposed that the black pumice strata are from the ME. The stratigraphic evidence shows that no apparent discontinuity exists between the gray-white pumice and the black pumice strata at the Tianwen peak (**Figures 5B–D**). The stratum in Baiyunfeng valley near the caldera turns from welded tuff to plastic beddings, then turning to welded tuff with bombs (**Figure 6D**). This stratigraphic evidence indicates a change during the ME, possibly with two eruption stages. The high-precision carbonized ages have been identified using the wiggle-match method, namely, A.D. 938–939 and 946 ± 3 (Yin et al., 2012; Xu et al., 2013). The carbonized woods reported in Yin et al. (2012) are from the north and south slopes, and carbonized wood reported in Xu et al. (2013) is from the west slope. The high-precision dating results also indicate a possibility that the strata of the carbonized wood are from different eruptive stages during the ME. The medial deposits have magma mixture characteristics (magma fragment strips in the gray-white pumice). However, most of the distal deposits are gray-white rhyolite, lacking evidence for a magma mixture. The above evidences show that the ME is likely to have at least two eruptive stages.

The grain-size distribution of the medial and distal strata in the PDCs shows a decrease in the median phi size (Md_{φ}) from top to bottom (**Figure 10**). Layers rich in lithics and large-particle pumices are mostly developed in the middle and lower parts (**Figures 8A–C**), which supports this result. However, this trend is affected by the physical properties of the clasts and the fluid properties of the PDCs. Pyroclasts with a high density and small particles are generally heavily affected by gravitational differentiation and are deposited at the bottom, such as lithic-rich layers. Pumices with a low density and large particles accumulate at the middle and upper parts in the distal stratum (**Figure 9B**). The turbulent movement of the ash cloud can carry large-particle pumices to the upper part. Lithic clasts increase when the thickness increases, while that of crystal clasts and glass clasts decreases. When the distance from the caldera increases, the content of lithics shows a decreasing trend (**Figure 10**). The changes in the content of lithics correlate with the vertical gravitational differentiation and the variation in the PDC density from the medial to the distal.

The PDCs during the ME, characterized by a large volume (approximately 7 km^3 in the Chinese territory), a high temperature (280–740°C), long run-out distances (50 km), and the ability to climb hills, experienced at least two stages, including an early rhyolite stage and a late trachyte stage. Magma mixing is common in the pumice. In China, Tianchi volcano is a famous scenic spot. Within 50 km around the volcano, there are three towns near the rivers with about 111,000 inhabitants (Ji, 2015). In 2019, about 2.47 million tourists visited Tianchi volcano park (Li, 2020). The strata of Tianwen Peak keep the evidence of several explosive eruptions (**Figure 5A**). Previous researchers proposed the ignimbrites forming stage of Tianchi volcano have occurred during the last 100,000 years (Jin and Zhang, 1994; Liu and Song, 1998; Liu, 2000). Although most of these eruptions lack clear age evidences, it is likely that the ignimbrite eruptions have some cycles. Nakada (2000) proposed that areas previously impacted by PDCs would be probably affected again in similar future eruptions. Therefore, the establishment of the PDC facies during the ME can guide the local government in construction planning and reducing hazardous affection of PDCs of potential future eruptions.

CONCLUSION

The ME PDCs form a pyroclastic apron that is thin at both ends and thick in the middle. When using the Tianchi caldera as the center, gully-type deposits formed within 0–10 km, valley-type deposits formed within 10–20 km, and fan-shape deposits formed within 20–50 km (**Figures 1D**, **14A,B**).

Stratigraphically, the PDC facies have the following characteristics. The proximal PDC deposits have eutaxitic and lava-like structures. The medial PDC strata include thick layer deposits, lithic-rich layers, pumice-rich layers, and columnar joints. The distal PDCs strata include coarse-tail layers, climbing layers, and ground surge layers. Gas escape structures also developed, among other structures. The degree of welding decreases with an increase in distance away from the caldera. The entire proximal strata are strongly welded in the vertical profiles, with a few being lava-like. The middle part of the medial strata is strongly welded and has a weakening welding degree at the upper and lower ends. The distal strata consist of loose deposits. Some of the distal deposits have been changed in to secondary lahar deposits by river flows.

The specific granulometric manifestation of the PDC facies are as follows: from the medial to distal strata, the change in media phi (Md_{φ}) indicates a decrease in the particle grain size; the reduction of the pyroclast content from the medial to distal strata demonstrates the gravitational differentiation of the PDCs.

The vertically lithofacies characteristics of the ME PDCs include (**Figure 14C**): lithofacies changes from welded tuffs of gray-black rhyolite with black trachytic components in the proximal deposits to partially welded tuffs of gray-black rhyolite (containing black trachytic components) in the medial deposits, followed by loose gray-white rhyolite in the distal PDC deposits.

The above results show that the PDC was a high-dense, high-energy fluid in the proximal strata with a low thickness. The PDC density decreases in the medial strata and had a weakened transportation that led to the formation of thick layers. An increasingly apparent gravitational differentiation effect was observed as the distance increases. The distal PDCs demonstrate strong fluidization characteristics and a density far lower than that of the proximal and medial strata, which shows a clear stratification.

The establishment of the PDC facies model assists in unraveling some PDCs emplacement processes, marked by a high

level of topography confinement, about 50 km runout distance, 280–750°C emplacement temperatures, and more than 7 km^3 volume, which provide insights of the PDCs destruction during the ME. In order to prevent potential PDCs hazard, newly constructed residential areas and tourism-related structures near Tianchi volcano should be at least 50 km away from the caldera, considering the effect of high temperatures and fire.

DATA AVAILABILITY STATEMENT

The raw data supporting the conclusions of this article will be made available by the authors, without undue reservation, to any qualified researcher.

AUTHOR CONTRIBUTIONS

BZ and JX: designing work plan. BZ and ZC: field geological survey and sampling. HY: microscopic rock slice identification and whole-rock analysis. BZ: scanning electron microscope (SEM) analysis. All authors contributed to the article and approved the submitted version.

FUNDING

This manuscript is jointly supported by the National Natural Science Foundation of China (41402299 and 41861144025) and the Fundamental Scientific Research Project of the Institute of Geology, China Earthquake Administration (IGCEA1516).

ACKNOWLEDGMENTS

The authors gratefully acknowledge the considerable effort by the editor and reviewers. Their valuable comments and constructive suggestions improved the manuscript substantially. The authors thank Professor Haiquan Wei and Professor Qingfu Yang for their guidance, the staff of Changbaishan Volcano Station and Longgang Volcano Station for their assistance in the field investigations, and Xiaomin Liao for the help of drawing.

REFERENCES

Bailey, R. A., and Carr, R. G. (1994). Physical geology and eruptive history of the Matahina Ignimbrite, Taupo volcanic zone, North Island, New Zealand. *J. Geol. Geophys.* 37, 319–344. doi: 10.1080/00288306.194.9514624

Baxter, P. J., Boyle, R., Cole, P., Neri, A., Spence, R., and Zuccaro, G. (2005). The impacts of pyroclastic surges on buildings at the eruption of the Soufrière Hills volcano, Montserrat. *Bull. Volcanol.* 67, 292–313. doi: 10.1007/s00445-004-0365-7

Bignami, C., Ruch, J., Chini, M., Neri, M., Buongiorno, M. F., Hidayati, S., et al. (2013). Pyroclastic density current volume estimation after the 2010 Merapi volcano eruption using X-band SAR. *J. Volcanol. Geotherm. Res.* 261, 236–243. doi: 10.1016/j.jvolgeores.2013.03.023

Blong, R. J. (1996). "Volcanic hazard risk assessment," in *Monitoring and Mitigation of Volcano Hazards*, eds R. Scarpa and R. I. Tilling (Berlin: Springer-Verlag), 675–698.

Branney, M. J., and Kokelaar, P. (2002). Pyroclastic density currents and the sedimentation of ignimbrite. *Lond. Memo. Geol. Soc.* 29–31, 115–118.

Cas, R. A. F., and Wright, J. V. (1987). *Volcanic Successions: Modern And Ancient*. London: Allen and Unwin.

Chen, X. W., Wei, H. Q., Yang, L. F., and Chen, Z. Q. (2017). Petrological and mineralogical characteristics of Tianchi Volcano, Changbai Mountain: implications for crystallization differentiation and magma mixing. *Acta Geoscientia Sin.* 38, 177–192. doi: 10.3975/cagsb.2017.02.11

Corsaro, R. A., Calvari, S., and Pompilio, M. (2005). Formation of lava stalactites in the master tube of the 1792-1793 flow field, Mt. Etna (Italy). *Am. Mineral.* 90, 1413–1421. doi: 10.2138/am.2005.1760

Cui, Z. X., Jin, D. C., and Li, N. (2000). The historical record discovery of 1999-1200 AD large eruption of Changbaishan tianchi volcano and its significance. *Acta Petrol. Sin.* 16, 191–193. doi: 10.3969/j.issn.1000-0569.2000.02.007

Cui, Z. X., Zhang, S. H., and Tian, J. (1997). The study on volcanic eruption and forest conflagration since Holocene in Changbai MT. *Geograph. Res.* 16, 92–97. doi: 10.11821/yj199701001

Druitt, T. H. (1998). Pyroclastic density currents. *Geol. Soc. Lond. Spec. Public.* 145, 145–182. doi: 10.1144/gsl.sp.1996.145.01.08

Dufek, J., Ongar, T. E., and Roche, O. (2015). "Pyroclastic density currents: processes and models," in *Encyclopedia of Volcanoes*, eds H. Sigurdsson, B. Houghton, S. R. McNutt, H. Rymer, and J. Stix (London: Academic Press), 617–629. doi: 10.1016/b978-0-12-385938-9.00035-3

Fan, Q. C., Liu, R. X., Wei, H. Q., Sui, J. L., and Li, N. (1999). Petrogeochemical characteristics of holocene eruption of Tianchi volcano, Changbai mountains. *Geol. Rev.* 45(Suppl.1), 263–271.

Fan, Q. C., Sui, J. L., Sun, Q., Li, N., and Wang, T. H. (2005). Preliminary research of magma mixing and explosive mechanism of the millennium eruption of Tianchi volcano. *Acta Petrol. Sin.* 21, 1703–1708. doi: 10.3321/j.issn:1000-0569.2005.06.017

Fan, Q. C., Sui, J. L., Wang, T. H., Li, N., and Sun, Q. (2006). Eruption history and magma evolution of the trachybasalt in Tianchi volcano, Changbaisha. *Acta Petrol. Sin.* 22, 1449–1457. doi: 10.3321/j.issn:1000-0569.2006.06.001

Fan, Q. C., Sui, J. L., Wang, T. H., Li, N., and Sun, Q. (2007). History of volcanic activity,magma evolution and eruptive mechanism s of the Changbai Volcanic Province. *Geol. J. China Univers.* 13, 175–190. doi: 10.3969/j.issn.1006-7493.2007.02.004

Horn, S., and Schmincke, H. U. (2000). Volatile emission during the eruption of Baitoushan Volcano (China/North Korea) ca. 969 AD. *Bull. Volcanol.* 61, 537–555. doi: 10.1007/s004450050004

Inman, D. L. (1952). Measures for describing the size distribution of sediments. *J. Sedimentol. Petrol.* 22, 125–145.

Jenkins, S., Komorowski, J. C., Baxter, P. J., Spence, R., Picquout, A., Lavigne, F., et al. (2013). The Merapi 2010 eruption: an interdisciplinary impact assessment methodology for studying pyroclastic density current dynamics. *J. Volcanol. Geotherm. Res.* 261, 316–329. doi: 10.1016/j.jvolgeores.2013.02.012

Ji, L. Y., Xu, J. D., Lin, X. D., and Luan, P. (2009). Application of satellite thermal infrared remote sensing in monitoring Changbaishan tianchi volcano activity. *Seismol. Geol.* 31, 617–627. doi: 10.3969/j.issn.0253-4967.2009.04.005

Ji, W. N. (2015). *The Evacuation Planning Research For The Millennium Eruption In Tianchi Volcano, Changbai, Mountains*. Master's thesis, Ocean University of China, Qingdao.

Jin, B. L., and Zhang, X. Y. (1994). *Researching Volcanic Geology In Mount Changbai*. Yanbian: Korean Ethnic Education Press.

Jin, D. C., and Cui, Z. X. (1999). A study of volcanic eruptions in Tianchi volcano, Changbai Mountains recorded in historical documents. *Geol. Rev.* 45(Suppl.1), 304–307.

Kyong-Song, R., Hammond, J. O. S., Chol-Nam, K., Hyok, K., Yong-Gun, Y., Gil-Jong, P., et al. (2016). Evidence for partial melt in the crust beneath Mt. Paektu (Changbaishan), democratic people's republic of Korea and China. *Sci. Adv.* 2:e1501513. doi: 10.1126/sciadv.1501513

Le Maitre, R. W. (1989). *A Classification Of Igneous Rocks And Glossary Of Terms*. Oxford: Blackwell Scientific Publications.

Lesti, C., Porreca, M., Giordano, G., Mattei, M., Cas, R. A. F., Wright, H. M. N., et al. (2011). High-temperature emplacement of the Cerro Galán and Toconquis group ignimbrites (Puna plateau, NW Argentina) determined by TRM analyses. *Bull. Volcano.* 73, 1535–1565. doi: 10.1007/s00445-011-0536-2

Li, J. T., and Sun, G. M. (1996). Recent volcanic activity in Changbaishan and regional earthquakes. *Seismol. Geomagnet. Observ. Res.* 17, 31–38.

Li, L. (2020). *Jilin Changbaishan Mountain Protection Development Management Committee*. Available online at: http://www.changbaishan.gov.cn/shjj/tjxx/202001/t20200102_145727.html (accessed January 15, 2020).

Liu, G. M., Sun, H. Y., and Guo, F. (2011). The newest monitoring information of Changbaishan volcano, NE China. *Acta Petrol. Sin.* 27, 2905–2911.

Liu, J. Q., Chen, S. S., Guo, W. F., Sun, C. Q., Zhang, M. L., and Guo, Z. F. (2015). Research advances in the Mt. Changbai volcano. *Bull. Mineral. Petrol. Geochem.* 34, 710–723. doi: 10.3969/j.issn.1007-2802.2015.04.005

Liu, J. Q., and Wang, S. S. (1982). The formation age of Changbaishan Tianchi volcano. *Sci. Bull.* 21, 1312–1315.

Liu, R. X. (2000). *Active Volcanoes in China*. Beijing: Seismological Press.

Liu, R. X., Fan, Q. C., Zheng, X. S., Zhang, M., and Li, N. (1998). "The products of the recent eruption from Tianchi volcano," in *The Recent Eruption of Tianchi Volcano, Changbaishan*, ed. R. X. Liu (Beijing: Science Press), 40–82.

Liu, R. X., Li, J. T., Wei, H. Q., Xu, D. M., and Zhen, X. S. (1992). Volcano at tianchi lake, Changbaishan MT. - a modern volcano with potential danger of eruption. *Acta Geophys. Sin.* 35, 661–665.

Liu, R. X., Qiu, S. H., Cai, L. Z., Wei, H. Q., Yang, Q. F., Xi, Z., et al. (1997). A study on the last major eruption of Tianchi volcano in Changbai Mountain and its significance. *Sci. China* 27:437. doi: 10.3321/j.issn:1006-9267.1997.05.005

Liu, R. X., and Song, S. R. (1998). "The eruptive history of Tianchi volcano," in *the recent eruption of Tianchi volcano, Changbaishan*, ed. R. X. Liu (Beijing: Science Press), 40–82.

Liu, R. X., Wei, H. Q., Tang, J., Song, S. R., and Li, X. D. (1996). Progress of the study on Tianchi volcano, Changbaishan, China. *Seismol. Geomagnet. Observ. Res.* 17, 2–11.

Liu, X. (1999). Tectonic control of cenozoic volcanism in Northeastern China. *World Geol.* 2, 23–29.

Liu, X. (2006). Sequence and distribution of the pyroclastic deposits of the greatest Eruption of Changbaishan volcano during the period of history. *J. Changchun Univer. Sci. Technol.* 36, 313–318. doi: 10.3969/j.issn.1671-5888.2006.03.001

Liu, X., and Xiang, T. Y. (1997a). *Cenozoic Volcanoes In Northeast China and Their Hazards Of Pyroclastic Deposits*. Changchun: Jilin University Press.

Liu, X., and Xiang, T. Y. (1997b). "Observation on the pyroclastic deposits from the 1000 years ago eruption of Tianchi volcano," in *The Volcanism And Human Environment*, ed. R. X. Liu (Beijing: Seismological Press), 14–20.

Liu, X., Xiang, T. Y., and Wang, X. K. (1989). Episodes of cenozoic volcanism in the Changbai Mountains area. *Jilin Geol.* 3, 30–41.

Loughlin, S. C., Calder, E. S., Clarke, A., Cole, P. D., Luckett, R., Mangan, M. T., et al. (2002). Pyroclastic flows and surges generated by the 25 June 1997 dome collapse, Soufrière Hills Volcano, Montserrat. *Geol. Soc. Lond. Mem.* 21, 191–209. doi: 10.1144/gsl.mem.2002.021.01.09

Luan, P. (2008). *A Study on Characteristics of Remote Sensing Images of Eruptive Products from the Tianchi Volcano in the Changbai Mountains*. Master's thesis, Institute of Geology, China Earthquake Administration, Beijing.

Machida, H., and Arai, F. (1983). Extensive ash falls in and around the Sea of Japan from large late quaternary eruptions. *J. Volcanol. Geotherm. Res.* 18, 151–164. doi: 10.1016/0377-0273(83)90007-0

Nakada, S. (2000). "Hazards from pyroclastic flows and surges," in *Encyclopedia Of Volcanoes*, ed. H. Sigurdsson (San Diego: Academic Press), 945–956.

Oppenhimer, C., Wacker, L., Xu, J. D., Diego Galván, J., Stoffel, M., Guillet, S., et al. (2017). Mult-proxy dating the 'millennium eruption' of Changbaishan to late 946 CE. *Q. Sci. Rev.* 158, 164–171. doi: 10.1016/j.quascirev.2016.12.024

Paladio-Melosantos, M. L. O., Solidum, R. U., Scott, W. E., Quiambao, R. B., Umbal, J. V., Rodolfo, K. S., et al. (1996). "Tephra falls of the 1991 eruptions of mount Pinatubo," in *Fire and Mud: Eruptions and Lahars of Mount Pinatubo, Philippines*, eds C. G. Newhall and R. S. Punongbayan (Seattle: University of Washington Press), 513–535.

Pan, B., De Silva, S. L., Xu, J. D., Chen, Z., Miggins, D. P., Wei, H., et al. (2017a). The VEI-7 Millennium eruption, Changbaishan-Tianchi volcano, China /DPRK: new field, petrological, and chemical constraints on stratigraphy, volcanology, and magma dynamics. *J. Volcanol. Geotherm. Res.* 343, 45–59. doi: 10.1016/j.jvolgeores.2017.05.029

Pan, B., Fan, Q. C., Xu, J. D., Wu, C. Z., Chen, Z. Q., and Guo, F. (2017b). Magmatic processes of the Millennium eruption at Changbaishan Tianchi volcano, China/North Korea. *Acta Petrol. Sin.* 33, 163–172.

Pierson, T. C., and Major, J. J. (2014). Hydrogeomorphic effects of explosive volcanic eruptions on drainage basins. *Annu. Rev. Earth Planet. Sci.* 42, 469–507. doi: 10.1146/annurev-earth-060313-054913

Shi, L. B., Chen, X. D., Yang, Q. F., Wei, H. Q., and Lin, C. Y. (2005). Petrochemistry of pumices of various colors produced by eruption of Changbaishan Tianchi volcano at 1000 years ago. *Seismol. Geol.* 27, 73–82. doi: 10.3969/j.issn.0253-4967.2005.01.008

Stone, R. (2010). Is China's riskiest volcano stirring or merely biding its time? *Science* 329, 498–499. doi: 10.1126/science.329.5991.498-a

Sui, J. L., Fan, Q. C., Liu, J. Q., and Guo, Z. F. (2007). Mantle heterogeneity beneath Changbaishan volcanic province: evidence from geochemical study on trace elements and isotopes. *Acta Petrol. Sin.* 23, 1512–1520.

Sulpizio, R., Dellino, P., Doronzo, D. M., and Sarocchi, D. (2014). Pyroclastic density currents: state of the art and perspectives. *J. Volcanol. Geotherm Res.* 283, 36–65. doi: 10.1016/j.jvolgeores.2014.06.014

Tang, Y., Obayashi, M., Niu, F. G., Grand, S. P., Chen, Y. J., Kawakatsu, H., et al. (2014). Changbaishan volcanism in Northeast China linked to subduction-induced mantle upwelling. *Nat. Geosci.* 7, 470–475. doi: 10.1038/ngeo2166

Wadge, G., Voight, B., Sparks, R. S. J., Cole, P. D., Loughlin, S. C., and Robertson, R. E. A. (2014). "An overview of the eruption of Sourfrière Hills Volcano, Montserrat from 2000 to 2010," in *The Eruption of Sourfrière Hills Volcano, Montserrat from 2000 to 2010*, eds G. Wadge, R. E. A Robertson, and B. Voight (London: Geological Society, London, Memoirs), 39, 1–39.

Wang, P. J., Jian, Y., Chen, C. Y., and Wang, Y. Q. (2013). Volcano-stratigraphy and volcanic architecture of the Changbaishan volcanos, NE China. *J. Jilin Univers.* 43, 319–339. doi: 10.13278/j.cnki.jjuese

Wang, Y. Q., Yu, H. M., Xu, J. D., Chen, Z. Q., and Zhao, B. (2019). A comparative study on the characteristics of two fallout pumices deposits from the millennium eruption of Tianchi volcano in Changbaishan area. *Seismol. Geol.* 41, 208–217. doi: 10.3969/j.issn.0253-4967.2019.01.014

Wei, H. Q. (2010). Magma upmoving process within the magma prism beneath the Changbaishan volcano. *Earth Sci. Front.* 17, 11–23.

Wei, H. Q. (2014). *Tianchi Volcano in the Changbai Mountains*. Beijing: Seismological Press.

Wei, H. Q., Hong, H., Sparks, R. S. J., Walder, J. S., and Bin, H. A. N. (2004a). Potential hazards of eruptions around the Tianchi Caldera lake, China. *Acta Geol. Sin.* 78, 790–794. doi: 10.3321/j.issn:1000-9515.2004.03.024

Wei, H. Q., Jin, B. L., and Liu, Y. S. (2004b). Some advance in the study of volcanic geology and a hazard analysis of Tianchi volcano. *Acta Petrol. Mineral.* 23, 305–312. doi: 10.3969/j.issn.1000-6524.2004.04.008

Wei, H. Q., Liu, G., and Gill, J. (2013). Review of eruptive activity at Tianchi volcano, Changbaishan, Northeast China: implications for possible future eruptions. *Bull. Volcanol.* 75, 1–14. doi: 10.1007/s00445-013-0706-5

Wei, H. Q., Liu, R. X., and Li, X. D. (1997). Ignimbrite-forming eruptions from Tianchi volcano and their climate effect. *Earth Sci. Front.* 4, 253–266.

Wei, H. Q., Liu, R. X., and Yang, Q. F. (1998). "Recovery of the dynamic process of ignimbrite formation in Tianchi volcano," in *The Recent Eruption of Tianchi Volcano, Changbaishan*, ed. R. X. Liu (Beijing: Science Press), 83–107.

Wei, H. Q., Wang, Y., Jin, J. Y., Gao, L., Yun, S. H., and Jin, B. L. (2007). Timescale and evolution of the intracontinental Tianchi volcanic shield and ignimbrite-forming eruption, Changbaishan, Northeast China. *Lithos* 96, 315–324. doi: 10.1016/j.lithos.2006.10.004

Wright, H. M. N., Lesti, C., Cas, R. A. F., Porreca, M., Viramonte, J. G., Folkes, C. B., et al. (2011). Columnar jointing in vapor-phase-altered, non-welded Cerro Galán Ignimbrite, Paycuqui, Argentina. *Bull. Volcano.* 73, 1567–1582. doi: 10.1007/s00445-011-0524-6

Wu, J. P., Ming, Y. H., Zhang, H. R., Liu, G. M., Fang, L. H., Su, W., et al. (2007). Earthquakes swarm acitivity in Changbaishan Tianchi volcano. *Chin. J. Geophys.* 50, 1089–1096.

Xu, J. D., Liu, G. M., Wu, J. P., Ming, Y. H., Wang, Q. L., Cui, D. X., et al. (2012). Recent unrest of Changbaishan volcano, Northeast China: a precursor of a future eruption? *Geophys. Res. Lett.* 39:L16305. doi: 10.1029/2012GL052600

Xu, J. D., Pan, B., Liu, T. Z., Hajdas, I., Zhao, B., Yu, H. M., et al. (2013). Climatic impact of the Millennium eruption of Changbaishan volcano in China: new insights from high-precision radiocarbon wiggle-match dating. *Geophys. Res. Lett.* 40, 54–59. doi: 10.1029/2012GL054246

Yang, Q. F., Li, J. T., Liu, R. X., and Sun, G. J. (1996). Physical mechanism of 750~960AD pumice-flow transport and deposit of Tianchi volcano, Changbajshan. *Seismol. Geomagnet. Observat. Res.* 7, 11–19.

Yang, Q. F., Shi, L. B., Zhang, Y., Chen, B., and Chen, X. D. (2007). Grain-size characteristics of the millennium pyroclastic flow deposits of Tianchi volcano and their geological implications. *Seismol. Geol.* 29, 480–491. doi: 10.3969/j.issn.0253-4967.2007.03.004

Yin, J. H., Timoth Jull, A. J., Burr, G. S., and Zheng, Y. G. (2012). A wiggle-match age for the millennium eruption of Tianchi volcano at Changbaishan, Northeastern China. *Q. Sci. Rev.* 47, 150–159. doi: 10.1016/j.quascirev.2012.05.015

Yin, J. H., Zheng, Y. G., and Liu, Y. X. (2005). The radiocarbon age of carbonized wood in Tianchi volcano, Changbaishan mountains and its implication. *Seismol. Geol.* 27, 83–88. doi: 10.3969/j.issn.0253-4967.2005.01.009

Yu, H. M., Wu, J. P., Xu, J. D., Lin, C. Y., Shi, L. B., and Chen, X. D. (2012). Microstructural characteristics of the Holocene pumice erupted from Changbaishan Tianchi volcano and their volcanological implications. *J. Jilin Univer.* 42(Suppl.3), 132–144.

Yu, H. M., Xu, J. D., Luan, P., Zhao, B., and Pan, B. (2013). Probabilistic assessment of tephra fallout hazard at Changbaishan volcano, Northeast China. *Nat. Hazards* 69, 1369–1388. doi: 10.1007/s11069-013-0683-1

Zhang, M. L., Guo, Z. F., Cheng, Z. H., Zhang, L. H., and Liu, J. Q. (2015). Late Cenozoic intraplate volcanism in Changbai volcanic field, on the border of China and North Korea: insights into deep subduction of the Pacific slab and intraplate volcanism. *J. Geol. Soc.* 172, 648–663. doi: 10.1144/jgs2014-080

Zhao, B., Xu, J. D., and Lin, C. Y. (2013). Study of distal pyroclastic-flow stratum from Tianchi volcano in 1215(±15)eruption: pyroclastic-flow over water. *Acta Geol. Sin.* 87, 73–81. doi: 10.1111/1755-6724.12031

Zou, H. B., Yang, Q. F., and Zhang, H. F. (2010). Rapid development of the great Millennium eruption of Changbaishan (Tianchi) volcano, China/North Korea: Evidence from U-Th zircon dating. *Lithos* 119, 289–296. doi: 10.1016/j.lithos.2010.07.006

Conflict of Interest: The authors declare that the research was conducted in the absence of any commercial or financial relationships that could be construed as a potential conflict of interest.